A Similarity Approach for an Unsteady Two-dimensional Forced Convective Heat Transfer Boundary Layer Flow along a Convergent Channel

M. S. Alam, Department of Mathematics, Jagannath University, Bangladesh

Correspondence:
M. S. Alam
Department of Mathematics, Jagannath University, Dhaka-1100, Bangladesh.
E-mail: dralamjnu@gmail.com

Abstract

The unsteady flow in a converging channel ("wedge nozzle") is analyzed in the present paper. A specific similarity approach is used, which leads to a model where the temporal and spatial variables are combined into a single parameter in the flow problem. In the second part of the paper the problem of convective heat transfer is analyzed. Considering a variable wall temperature, there are two possibilities identified, leading to similarity solutions, namely a linear or an inverse linear wall temperature. Only the second case produces physical solutions. Numerical results are given in terms of skin friction and Nusselt number variations along the wedge nozzle and velocity and temperature boundary layer distributions. The obtained numerical results show that the skin friction increases along the wedge nozzle for positive values of unsteadiness parameter while it decreases for negative values of unsteadiness parameter. Results also show sharp variations in the streamwise direction of the Nusselt number, for larger values of the unsteadiness parameter.

Keywords: Wedge nozzle, unsteady flow, forced convection, boundary layer.

1. Introduction

We consider in this paper the unsteady flow in a converging channel ("wedge nozzle"), formed between two intersecting planes as shown in Fig. 1. This problem, studied originally by Pohlhausen [1] for the steady case, refers to a pressure gradient driven flow, whose main-stream velocity varies inversely with the coordinate along the channel flow. A contemporary reference where the wedge nozzle problem is presented in a more general framework is the textbook by Schlichting and Gersten [2].

With the x coordinate chosen as the distance from the line of intersection of the planes, similarity solutions of the boundary layer equations may be obtained if the velocity distribution $U(x)$ of the inviscid outer flow is of power-law type, which is characteristic for so-called wedge flows. One of the flows belonging to this class is the flow in a convergent channel (sink flow), where $U(x) = -a/x$. If $a > 0$ this velocity distribution describes a flow directed toward the line of intersection of the planes.

In this case, a backward boundary layer flow will develop, according to Goldstein [3]. This problem was revisited by Magyari [4], who studied the Pohlhausen problem with heat transfer, with a prescribed power-law variation of the wall temperature.

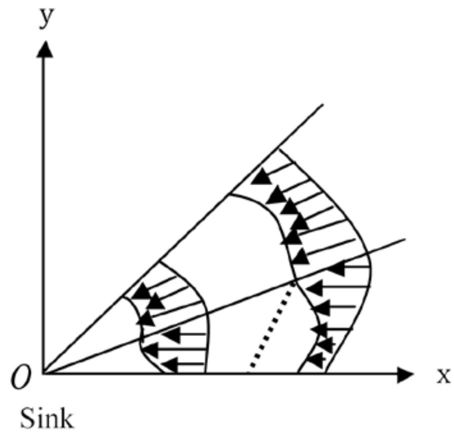

Fig. 1. Flow configuration and coordinates system.

The present paper is the counterpart of Magyari's study, in unsteady conditions. Unlike in that paper, where a fine full analytical approach was carried out, our case uses numerical solutions, also in the framework of similarity solutions.

2. Flow dynamics and similarity analysis

We consider an unsteady two-dimensional hydrodynamic laminar boundary layer flow of a viscous incompressible fluid in a convergent channel. With the *x*-axis chosen as explained in the introductory section and the *y*-axis taken normal to it, the governing equations are those of continuity and momentum (see also Mia et al.[5])

$$\frac{\partial u}{\partial x} + \frac{\partial v}{\partial y} = 0, \tag{1}$$

$$\frac{\partial u}{\partial t} + u\frac{\partial u}{\partial x} + v\frac{\partial u}{\partial y} = -\frac{1}{\rho}\frac{\partial p}{\partial x} + \frac{\partial^2 u}{\partial y^2}, \tag{2}$$

with boundary conditions

$$u = 0, v = 0 \text{ at } y = 0, \tag{3a}$$

$$u = U(x, t) \text{ as } y \rightarrow \infty, \tag{3b}$$

where (u, v) are the velocity components along (x, y) directions, t is the time, p is the pressure, ρ is the fluid density, υ is the kinematic viscosity, and $U(x, t)$ is the potential velocity.

In a certain analogy with Magyari [4], who took for the steady problem $U(x) = U_0 L/x$, where L is a reference length defined as that x-distance where the main stream velocity is U_0, we consider here the potential flow velocity generated by a convergent channel as

$$U(x, t) = -\frac{U_0\delta}{x}, \tag{4}$$

where U_0 is taken as positive, according to the introductory discussion and δ is a time dependent similarity quantity $\delta = \delta(t)$, which has the unit of a length. It appears that the idea to introduce such an expression of the flow unsteadiness was proposed by Birkhoff [6] and used in a series of papers by Sattar and co-workers [7-10].

Since the potential flow velocity is a function of x and t, the inviscid momentum equation outside the boundary layer is

$$\frac{1}{\rho}\frac{\partial p}{\partial x} = \frac{\partial U}{\partial t} + U\frac{\partial U}{\partial x} = -\frac{U_0}{x}\frac{d\delta}{dt} - \frac{U_0^2\,\delta^2}{x^3}. \tag{5}$$

In order to obtain similarity solutions of the problem, we now introduce the transformation

$$\psi = -\sqrt{\upsilon U_0\delta}\, f(\eta),\ \eta = \frac{y}{x}\sqrt{\frac{U_0\delta}{\upsilon}} \tag{6}$$

where ψ is the stream function that satisfies the continuity equation (1). Thus, the velocity components are obtained as

$$u = \frac{\partial\psi}{\partial y} = -\frac{U_0\delta}{x} f',\ v = -\frac{\partial\psi}{\partial x} = -\frac{\sqrt{U_0\upsilon\delta}}{x}\eta f' \tag{7}$$

Now using (5) and (7) into (2), we obtain

$$f''' - (f')^2 + 1 + A\,(2 - 2f' - \eta f'') = 0\ . \tag{8}$$

The boundary conditions are transformed as

$$f = 0, f' = 0 \ \text{ at }\ \eta = 0 \tag{9a}$$

$$f' = 1,\ \text{ as }\ \eta \to \infty, \tag{9b}$$

where prime denotes differentiation with respect to the variable η and

$$A = \frac{x^2}{2U_0\delta^2}\ \frac{d\delta}{dt} = \frac{X^2}{2\Delta^2}\ \frac{d\Delta}{d\tau}. \tag{10}$$

The following dimensionless spatial and temporal variables

$$\Delta = \frac{\delta}{L}, X = \frac{x}{L}, \tau = \frac{U_0}{L}t \tag{11}$$

have been introduced, where L is a characteristic length.

We remark that the parameter A contains a combination of the spatial and temporal coordinates, as the single parameter left in the problem.

Further, the wall shear stress is given by

$$\tau_w = -\mu\left(\frac{\partial u}{\partial y}\right)_{y=0} = \frac{\mu U_0\delta}{x^2}\sqrt{\frac{U_0\delta}{\upsilon}}\ f''(0). \tag{12}$$

Here the negative sign is due to the fact that the flow is in the opposite direction to the positive x-axis. Therefore the local skin-friction coefficient is obtained as

$$C_{fx} = \frac{\tau_w}{\frac{1}{2}\rho U^2\ (x,t)} = 2(\mathrm{Re}_\delta)^{-1/2} f''(0), \tag{13}$$

where $\mathrm{Re}_\delta = U_0\delta/\upsilon$ is a local Reynolds number. This non-conventional (modified) Reynolds number may be related to the usual local Reynolds number $\mathrm{Re}_x = U_0 x/\upsilon$ through the relationship $\mathrm{Re}_\delta = (\delta/x)\,\mathrm{Re}_x$.

3. Heat transfer

The energy equation is

$$\frac{\partial T}{\partial t} + u\frac{\partial T}{\partial x} + v\frac{\partial T}{\partial y} = \alpha\frac{\partial^2 T}{\partial y^2}, \tag{14}$$

when buoyancy, as well as other effects, such as viscous dissipation are neglected, as in Magyari [4]. Usual notations are used for T (fluid temperature) and α (thermal diffusivity). The boundary conditions are

$$T = T_w(x, t) \text{ at } y = 0, \tag{15a}$$

$$T \to T_\infty \text{ as } y \to \infty. \tag{15b}$$

The wall temperature is taken as

$$T_w(x, t) = T_\infty + (T_0 - T_\infty)\, h(x, t), \tag{16}$$

where $h(x,t)$ is a dimensionless function to be found by requiring similarity solutions. Besides the similarity variable η defined in (6), we introduce

$$T(x, t) = T_\infty + (T_0 - T_\infty)\, h(x, t)\, \theta(\eta). \tag{17}$$

Energy equation (14) becomes

$$\frac{1}{\Pr} h \frac{U_0\delta}{x^2}\theta'' \frac{\eta}{2\delta}\frac{d\delta}{dt} h\theta' + \frac{U_0\delta}{x}\frac{\partial h}{\partial x} f'\theta - \frac{\partial h}{\partial t}\theta = 0 \tag{18}$$

Imposing the proportionality of the coefficients of the first and third term in (18), two possible cases are found, which are discussed below:

(a) $h = C_1 x$, where $C_1 = C_1(t)$ has the dimension of a $(\text{length})^{-1}$. In this case (18) becomes

$$\frac{1}{\Pr}\theta'' + f'\theta - \frac{x^2}{2U_0\delta}\left(\frac{1}{\delta}\frac{d\delta}{dt}\eta\theta' + \frac{2}{C_1}\frac{dC_1}{dt}\theta\right) = 0, \tag{19}$$

and it follows that $C_1 = \delta / L^2$ in order to get similarity solutions and to satisfy the appropriate dimensionality of C_1. Finally, we get

$$\frac{1}{\Pr}\theta'' + f'\theta - A(\eta\theta' + 2\theta) = 0 \tag{20}$$

and the temperature distribution is given by

$$T(x,t) = T_\infty + (T_0 - T_\infty)\frac{\delta x}{L^2}\theta(\eta) = T_\infty + (T_0 - T_\infty) + \Delta X\theta(\eta), \tag{21}$$

where the quantity A is defined in (10).

(b) $h = C_2 / x$, where $C_2 = C_2(t)$ has the dimension of a length. In this case (20) becomes

$$\frac{1}{\Pr}\theta'' + f'\theta - \frac{x^2}{2U_0\delta}\left(\frac{1}{\delta}\frac{d\delta}{dt}\eta\theta' + \frac{2}{C_2}\frac{dC^2}{dt}\right)\theta = 0, \tag{22}$$

and it follows the natural choice $C_2 = \delta$ in order to get similarity solutions and to satisfy the appropriate dimensionality of C_2. Finally, we get

$$\frac{1}{\Pr}\theta'' - f'\theta + A(\eta\theta' + 2\theta) = 0 \tag{23}$$

and the temperature distribution is given by

$$T(x,t) = T_\infty + \frac{(T_0 - T_\infty)\delta}{x}\,\theta(\eta) = T_\infty + \frac{(T_0 - T_\infty)\,\Delta}{X}\,\theta(\eta). \tag{24}$$

Equations (20) and (23) may be written in the unified form

$$\frac{1}{\Pr}\theta'' + s\,[\,f'\theta - A\,(\eta\theta' + 2\theta)] = 0, \tag{25}$$

where s = 1 stands for case (a), i.e. linear wall temperature variation and s = -1 signifies inverse linear wall temperature variation as described by case (b). Equation (25) must be solved along the boundary conditions:

$$\theta(0) = 1,\ \theta(\infty) = 0 \tag{26}$$

Furthermore, the wall heat flux is given by

$$q_w = -k\left(\frac{\partial T}{\partial y}\right)_{y=0} = -k\,(T_0 - T_\infty)\frac{h(x,t)}{x}\sqrt{\frac{U_0\delta}{\upsilon}}\,\theta'(0). \tag{27}$$

Therefore the local Nusselt number is ($Nu_x = xq_w / k(T_w - T_\infty)$) becomes, on using (16),

$$Nu_x = -\,(\mathrm{Re}_\delta)^{1/2}\,\theta'(0), \tag{28}$$

irrespective of the choice of the function h.

4. Analytical solution for steady case

In steady flow (A = 0, i.e. K = 0) the momentum equation (8) becomes

$$f''' + 1 - f'^2 = 0 \tag{29}$$

which, subjected to (9), has the analytic solution

$$f'(\eta) = -2 + 3\tanh^2\xi, \text{ where } \xi = \frac{\eta}{2} + \tanh\left(\sqrt{\frac{2}{3}}\right) \tag{30}$$

obtained by Pohlhausen [1]. From (30) one has $f''(0) = \sqrt{4/3}$.

5. Numerical solutions

The boundary value problems (8-9) and (25-26) have been solved using comparatively the routines *bvp4c* and *dsolve* from Matlab [11] and Maple [12] packages, respectively.

5.1 Flow dynamics

In a first step, we tested the numerical method for K = 0 and we obtained $f''(0)$ = 1.1547005 which is identical to the value obtained analytically: $f''(0) = \sqrt{4/3}$ see equation (30).

Consequently, all curves in Fig. 2, which give the skin-friction group $C_{fx}\,(\mathrm{Re}_\delta)^{1/2}/2 = f''(0)$, start from the common point $(0, \sqrt{4/3})$. The trends are evident: the skin friction increases along the wedge nozzle for positive K and decreases for negative K.

In Fig. 3 there are plotted some samples of velocity profiles for K = -0.5. There is a small effect of X on these velocity distributions in the boundary layer. Fig. 4 is also for velocity profiles, this time represented at X = 1. Included also for reference in this figure is the curve corresponding to steady

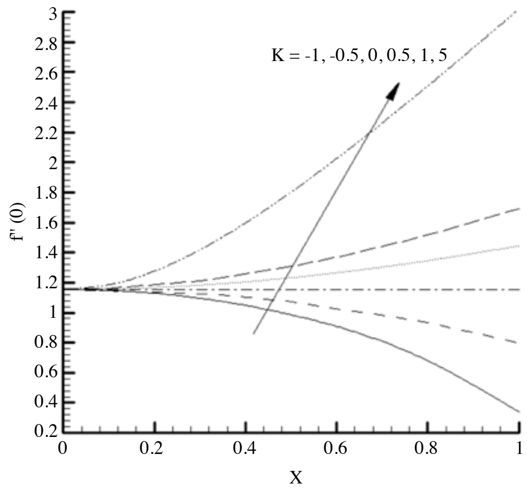

Fig. 2. Streamwise skin-friction variation for several values of the unsteadiness parameter *K*.

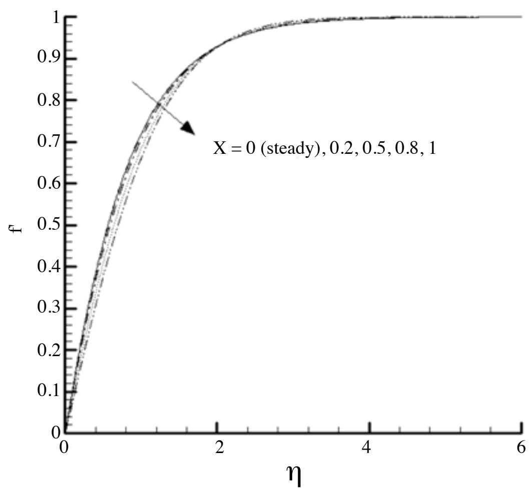

Fig. 3. Dimensionless velocity profiles for different values of *X* at *K* = -0.5.

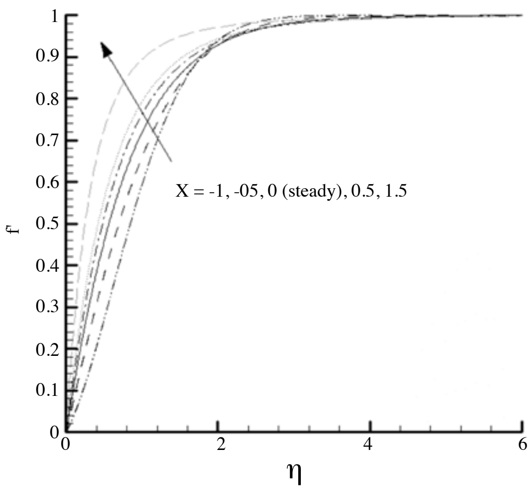

Fig. 4. Dimensionless velocity profiles for different values of *K* at *X* = 1.

conditions (for $K = 0$, i.e. $A = 0$). The influence of the unsteadiness parameter on the velocity profiles is evident in Fig. 4. We point out that no backward flows were detected in this analysis.

5.2. Heat transfer

Results for the heat transfer are obtained by solving (25-26), and $f'(\eta)$ is known from the previous step. Besides the parameter A from the momentum equation, there is also the Prandtl number Pr to be prescribed for the heat transfer problem. We have two options: linear or inverse linear wall temperature distributions. From the physical side, the linear case is easier to be understood than the inverse linear one. However, the second one is also encountered in the literature.

Equation (25) cannot be solved analytically, but further insight is obtained by the following procedure: multiplying (25) by θ', integrating once and using the boundary conditions (26) yields

$$\int_{\eta}^{\infty} f'\,\theta\theta\, d\eta = \frac{s}{2\mathrm{Pr}}\,\theta'^2 + \theta^2 + A\int_{\eta}^{\infty} \eta\theta'^2\, d\eta \qquad (33)$$

It is evident that the last term in the RHS is positive, while LHS is negative, as can easily be demonstrated. This leads to the conclusion that when $s = 1$ and $A > 0$ (i.e. $K > 0$) the solution of (25) does not exist.

Moreover, the numerical runs, performed with both Maple and Matlab solvers, prove that the case $s = 1$ (linear wall temperature) and $K < 0$ cannot be achieved, from the physical point of view, giving unrealistic temperature profiles.

Consequently, the following results are reported for the case of inverse linear wall temperature distribution ($s = -1$). Some samples of the streamwise variation of the Nusselt number are shown in Fig. 5, for two typical values of Pr = 0.7 and Pr = 7. Our numerical runs prove that, except for very small values of K (in absolute value), sharp variations of the Nusselt number, as given by $[-\theta'(0)]$, occur. These jumps appear in several locations along the channel length, and these locations are more numerous as the unsteadiness parameter K increases (in absolute value). This is the reason to interrupt the curves in Figs. 5 and 6. Otherwise, for both Pr = 0.7 and Pr = 7, the overall trend of the Nusselt number is to decrease in the streamwise direction for $K < 0$, and conversely for positive K (not shown in figures).

Finally in Fig. 6 we observe that the temperature profiles are found to decrease with the increasing values of the Prandtl number.

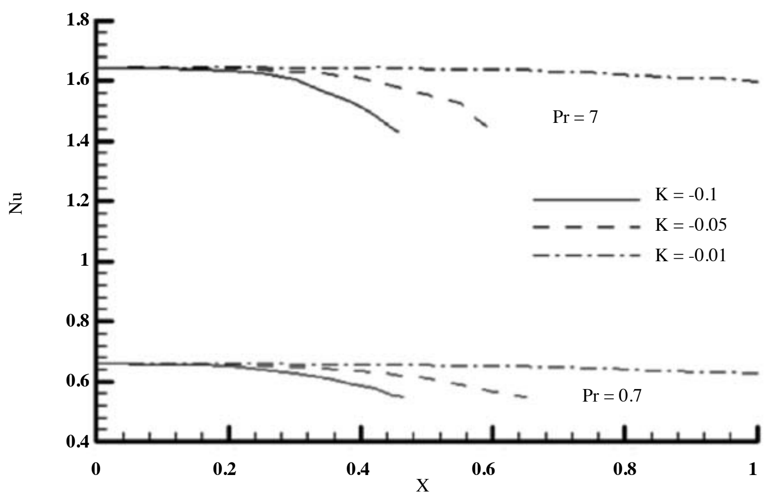

Fig. 5. Streamwise Nusselt number variation, inverse linear wall temperature distribution.

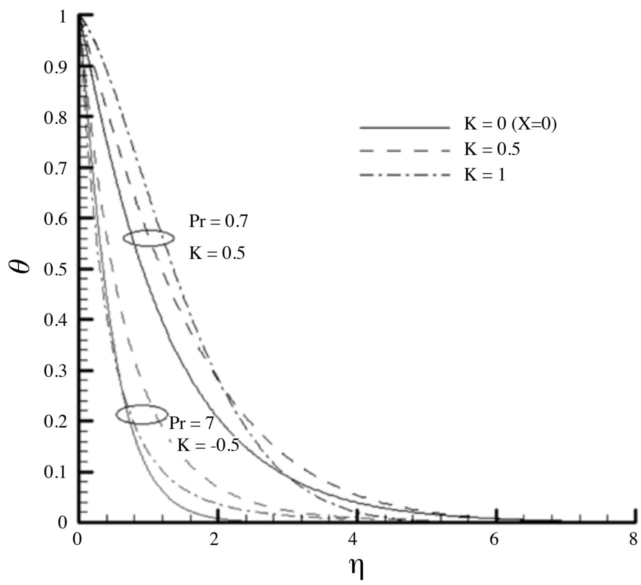

Fig. 6. Dimensionless temperature profiles for several values of *Pr* and *K*.

6. Concluding remarks

In this paper, local similarity solutions for the heat transfer flow along a convergent channel have been obtained only when the wall temperature is a linear or inverse linear function of x. No solutions exist for the temperature in the first case. Extensive numerical computations have been carried out for the second case, using two solid solvers, namely *bvp4c* and dsolve from Matlab and Maple packages, respectively. Both of them gave the result of sharp variations in the streamwise direction of the Nusselt number, for larger values of the unsteadiness parameter, but no anomalies were detected in the temperature profiles.

7. Acknowledgement

The author wish to thank the anonymous referee for his valuable comments for further improvement of the paper.

8. References

[1] Pohlhausen, K., Zur naherungsweisen Integration der Differentialgleichung der laminaren Grenzschicht. J. Appl. Math. Mech. (ZAMM), Vol. 1, pp. 252-268, 1921.

[2] Schlichting, H., Gersten, K., Boundary layer theory, 8th Edition, Springer-Verlag Berlin Heidelberg, p. 174, 2000.

[3] Goldstein, S., On backward boundary layers and flow in converging passages. J. Fluid Mech. Vol. 21, pp. 33-45, 1965.

[4] Magyari, E., Backward boundary layer heat transfer in a converging channel. Fluid Dyn. Res. Vol. 39, pp. 493-504, 2007.

[5] Mia, M. M. Sattar, M. A., Alam, M. S., A local similarity solution for unsteady two-dimensional hydrodynamic boundary layer flow in a convergent channel, Int. J. Energy and Technology, Vol. 3(7), pp. 1-4, 2011b.

[6] Birkhoff, G., Hydrodynamics. A study in Logic, Fact, and Similitude. Second edition, revised and enlarged, 2nd ed, Princeton University Press, Princeton, 1960.

[7] Sattar, M.A., Hossain, M.M., Unsteady hydromagnetic free convection flow with Hall current and mass transfer along an accelerated porous plate with time dependent temperature and concentration. Can. J. Phys. Vol. 70, pp. 369-374, 1992.

[8] Sattar, M.A., Unsteady hydromagnetic free convection flow with Hall current mass transfer and variable suction through a porous medium near an infinite vertical porous plate with constant heat flux.. Int. J. Energy Research, Vol. 18, pp. 771-775, 1994.

[9] Alam, M. S., Sattar, M. A., Rahman, M. M., Postelnicu, A., Local similarity solutions of ajn unsteady hydromagnetic convection flow of a micropolar fluid along a continuously moving permeable plate, Int. J. Heat and Technology, Vol. 28(2), pp. 95-105, 2010.

[10] Sattar, M. A., A local similarity transformation for the unsteady two-dimensional hydrodynamic boundary layer equations of a flow past a wedge, Int. J. Appl. Math. and Mech., Vol. 7(1), pp. 15-28, 2011a.

[11] Matlab 6.00 Mathworks, Inc., 2000.

[12] Maple 8.00 Waterloo Maple, Inc., 2002.